Magneto-optics of InAs/$Ga_{1-x}In_xSb$ infrared superlattice diodes

F. Fuchs,[a] E. Ahlswede, U. Weimar, W. Pletschen, and J. Schmitz
Fraunhofer-Institut für Angewandte Festkörperphysik (IAF), Tullastrasse 72, D-79108 Freiburg, Germany

M. Hartung and B. Jager
Sektion Physik der Ludwigs-Maximilian-Universität München, Geschwister-Scholl-Platz 1, 80539 München, Germany

F. Szmulowicz
Air Force Research Laboratory, Wright Patterson AFB, Ohio 45433-7707

(Received 15 June 1998; accepted for publication 20 October 1998)

Spectrally resolved measurements of the responsivity of infrared photodiodes based on InAs/(GaIn)Sb superlattices (SL) were performed in applied magnetic fields. For the field oriented parallel to the growth axis, interband Landau transitions related to both the center and the edge of the SL Brillouin zone in the growth direction were observed, in accordance with the parity selection rules that are expected for the type II system under consideration. For the field oriented perpendicular to the growth axis, the interband Landau resonances are broadened and the widening of the band gap is smaller. © *1998 American Institute of Physics.* [S0003-6951(98)04751-2]

InAs/(GaIn)Sb superlattices (SLs) show a broken-gap type-II band alignment.[1] For short period superlattices with sufficiently thin individual layers, confinement and strain effects result in an effective band gap which is tunable between zero and about 0.3 eV.[1] The realization of infrared (IR) detectors,[2,3] as well as lasers,[4] operating in the midinfrared has been reported. In low gap photodiodes the major source of leakage currents are tunneling currents.[3] The magnitude of interband-tunneling currents depends on the effective masses of the carriers involved, the size of the depletion layer, and the band gap. By applying a magnetic field, the tunneling currents can be reduced in a manner that is found to be strongly dependent on the field orientation.[5,6] In order to understand such tunneling experiments correctly, it is necessary to know the effective masses and the band gap as a function of the applied magnetic field. In the present letter we report on spectrally resolved measurements of the photoresponse of infrared photodiodes based on InAs/(GaIn)Sb SLs. The spectra were recorded by applying magnetic fields oriented parallel to the built-in electric field E of the diode (parallel to the growth axis) as well as perpendicular to the E field. By directly observing the interband Landau transitions, we find a strong anisotropic widening of the band gap. In addition, we discover higher lying transitions related to the SL Brillouin zone (BZ) boundary at $q_z=\pi/d$ (where d is the SL period) and compare them with state-of-the-art calculations.

The investigated diodes comprise a 150-period SL consisting of 39 Å InAs and 25-Å-thick $Ga_{0.85}In_{0.15}Sb$ layers grown by solid-source molecular-beam epitaxy on GaSb substrates. Details about growth conditions, diode design, and processing and performance have been published in Refs. 3 and 7.

Table I shows the results of a 8×8 kp band structure calculation[8] using the input parameters of the present SL structures as determined by high-resolution x-ray diffraction. The residual mismatch to the GaSb substrate was -2.6×10^{-3}. Energies are given relative to the unstrained bulk InAs conduction band. In order to obtain the miniband width the energies at $q=0$ and $q_z=\pi/d$ are given. Furthermore, the effective masses for motion along the growth axis and in the layer plane are listed. A band overlap between the GaSb valence band maximum and the InAs conduction band minimum of 140 meV was used.[1] Typically, in InAs/(GaIn)Sb SLs a very strong mass anisotropy of the HH1 band is found: For motion in the layer plane, the effective hole mass is comparable to the effective electron mass while the hole dispersion for the motion along the SL growth axis yields a very heavy mass. In contrast, the anisotropy of the electron mass is small. The increase in the electron mass for motion along the growth direction is about 17%.

In Table II the transition energies and the parity selection rules for optical dipole transitions for wave vectors $q=0$ and $q_z=\pi/d$ are given. For a type II SL structure the parity selection rules for wave vectors $q=0$ and $q_z=\pi/d$ interchange compared to a type I structure, e.g., at $q=0$ (like in type-I SLs), (HHn,LHn) to Cm transitions with $m+n$ = even are allowed, while at $q_z=\pi/d$ (unlike in type-I SLs) $m+n$ must be odd.[9] Although transitions forbidden at symmetry points become allowed away from these points, the interband density of states is greatest at points of high sym-

TABLE I. Energies of the present InAs/(GaIn)Sb SL according to a 8×8 kp calculation. The values are given relative to the bulk InAs conduction band minimum. Individual layer thicknesses were 39.33 Å for the InAs layers and 24.65 Å for the $Ga_{0.85}In_{0.15}Sb$ layers.

Band	$q=0$ (meV)	$q_z=\pi/d$ (meV)	Miniband width (meV)	$m_\parallel^*$	m_z^*	m_{red}
C1	239	379	140	0.0235	0.0275	
HH1	91	91	0.05	−0.0342	−79.82	0.014
LH1	−109	−233	124	−0.278	−0.0302	0.022
HH2	−223	−221	2	−0.283	−1.741	0.022
C2	848	657	191	⋯	⋯	

[a]Electronic mail: ffuchs@iaf.fhg.de

TABLE II. Zero-field transition energies at the center of the SL-Brillouin zone ($q=0$) and for at the zone boundary along the growth direction ($q_z=\pi/d$) according to the calculated values shown in Table I. In addition, the parity selection rules of the type II SL system are given as + for allowed and − for forbidden.

$\Delta E(q=0)$ (meV)	Selection rule	$\Delta E(q_z=\pi/d)$ (meV)	Selection rule
C1–HH1:148	+	C1–HH1:288	−
C1–LH1:348	+	C1–LH1:612	−
C1–HH2:462	−	C1–HH2:600	+
C2–HH1:757	−	C2–HH1:566	+

metry, which gives rise to pronounced structure in interband magneto-optical spectra at those points.

Figure 1 (left panel) shows the photovoltaic response with the magnetic field oriented parallel to the built-in electric field E of the diode. The right panel of Fig. 1 shows the spectra divided by the zero-field spectrum on an expanded scale. The left panel shows a strong shift of the band edge to higher transition energies with increasing magnetic field in accordance with results obtained in earlier magnetotransmission experiments.[10] The structureless zero-field spectrum coalesces into pronounced resonances. At higher magnetic fields, new transitions appear around 0.35 and 0.58 eV and undergo a smaller shift in comparison to the band-gap-related transitions (right panel).

The energy positions of the spectral features versus magnetic field shown in Fig. 1 are plotted in Fig. 2. Arrows indicate the expected values of the zero-field transition energies at $q=0$ and $q_z=\pi/d$ based on the theoretical values shown in Table I. The transitions can be separated into two groups: The most prominent features near the band gap are attributed to interband-Landau transitions at $q=0$ between the conduction band C1 and the HH1 valence band, covering the spectral range between 0.15 and 0.3 eV. Within the first group some additional weak features are observed and may be attributed to spin splitting. The second group consists of features observed at higher energies, very close to the energies where transitions with $q_z=\pi/d$ are expected. Note, that

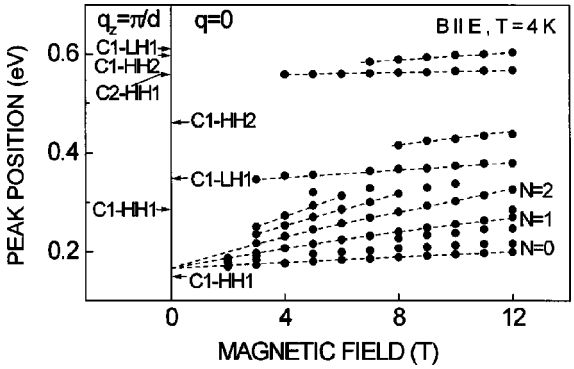

FIG. 2. Fan chart of the observed peak positions vs magnetic field for a B field oriented parallel to the built-in E field of the device. The expected zero-field transition energies at the center of the SL-Brillouin zone and at $q_z=\pi/d$ are indicated.

they are allowed according the selection rules listed in Table II.

The C1–HH2 transition is parity forbidden at the BZ center but parity allowed at $q_z=\pi/d$. Indeed, at 460 meV no spectral signature is observed, whereas between 560 and 610 meV two features appear, which can be identified as transitions at the BZ zone boundary along the z direction. The converse situation holds for the C1–HH1 transition, which is clearly observed at the BZ center with Landau indices ranging from 0 to 4, while at the expected energy for transitions with $q_z=\pi/d$ no signature is seen.

The energy shifts of the three dominant Landau transitions versus magnetic field for the motion of the hole and electron in the layer plane have been evaluated following the approach of Ref. 10. We obtain an effective reduced mass of 0.017, which is close to the value of 0.014 expected from the band structure calculation for the C1–HH1 transition at Γ (Table I). The remaining difference is attributed to the limited accuracy in the calculation of the effective hole mass because of the complicated dispersion of the valence band and the imprecise knowledge of band input parameters.

Figure 3 shows a comparison of the photoresponse for a B field oriented perpendicular to the E field of the diode (dashed lines) and the spectra obtained in the experimental

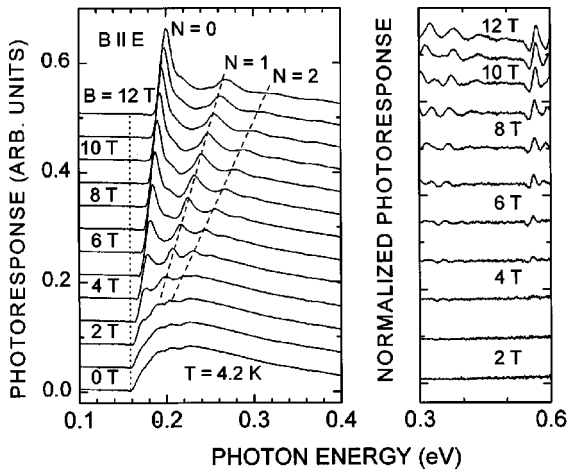

FIG. 1. Photoresponse of an InAs/(Galn)Sb SL diode with the magnetic field oriented parallel to the built-in electric field of the diode. The left panel shows the raw data, while in the right panel the high-energy part of the spectra divided by the zero-field spectrum is shown on expanded scale.

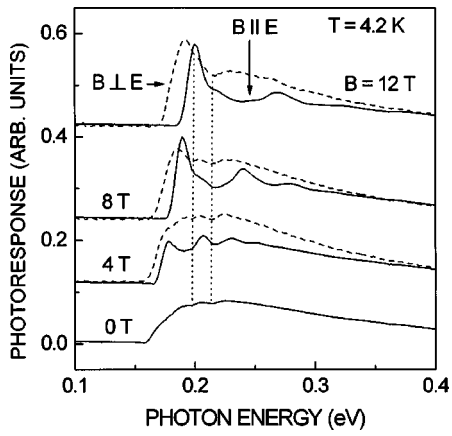

FIG. 3. Comparison of the photoresponse of an InAs/(Galn)Sb SL diode with magnetic fields oriented parallel (full lines) and perpendicular (dashed lines) to the built-in E field of the device. The spectral structures at 0.2 and 0.22 eV are due to the organic glue used for mounting of the samples (dotted lines). The inset shows the high-energy part of the zero-field spectrum on expanded scale.

configuration discussed earlier ($B\|E$, full lines). In contrast to the $B\|E$ orientation, the rich spectral structure vanishes and only one pronounced line at the band edge can be observed. The spectral features observed at 0.2 and 0.22 eV indicated with dotted lines are due to the organic glue used for sample mounting. The field-induced energy shift of the fundamental band gap for a B field oriented perpendicular to the E field is about half that for the parallel orientation. Applying the same evaluation as for the $B\|E$ orientation yields a reduced effective mass of 0.041.

The cyclotron mass measured with the magnetic field perpendicular to the E field is the geometric mean of the transport mass along two orthogonal directions.[11] The geometric mean of $m_{\|}$ and m_z of Table I yields an effective electron mass of 0.025 for that motion. This value gives an upper limit for the reduced effective mass. Any finite effective hole mass yields a smaller reduced mass. The geometric mean of the hole mass gives a value of 1.65 and can be neglected. Thus, with the experimental value of 0.041 for the geometric mean, the electron effective mass for the motion along the z direction equals $0.041^2/0.0235=0.07$ which is a factor of 3 higher than expected.

With the magnetic field perpendicular to the E field the motion of the carriers takes place in a plane containing the growth axis, in which the carriers are forced to move in the direction of the SL confinement. For a system of strongly coupled quantum wells, the condensation of the electronic structure into Landau levels is possible for Landau energies less than the miniband width,[11] which is fulfilled for both experimental configurations (see Table I). Maan[11] pointed out that such a condensation into Landau levels is associated with the unperturbed motion in closed cyclotron orbits. A perturbation of the orbits either due to reflection or scattering induces a line broadening.

The magnetic length at 1 T is about 80 nm, corresponding to 12 SL periods. At that field strength an electron performing a closed cyclotron orbit must cross the SL interfaces about 50 times. We tentatively attribute the broadening of the spectral structure with interface roughness scattering which is known to be the mechanism which limits the mobility in the present SL system.[12] The high value of the reduced mass in that experimental configuration may be caused by the stronger nonparabolicity for the electron dispersion along the z direction.

In summary, the anisotropy of the magnetic field induced widening of the band gap of InAs/(GaIn)Sb infrared photodiodes and the corresponding reduced effective masses have been determined. With the magnetic field oriented parallel to the E field, cyclotron orbits in the SL layer plane are induced and interband Landau transitions are observed. The widening of the band gap with the B field oriented parallel to the E field is consistent with the reduced effective mass obtained from 8×8 kp band structure calculations. At higher B fields, higher lying transitions at wave vectors $q_z=\pi/d$ become observable (i) at the calculated energy positions and (ii) in accordance with the parity selection rules that are expected for the type II system under consideration. With the B field oriented perpendicular to the E field, the rich spectral structure observed in the parallel configuration disappears and the widening of the gap is reduced.

The authors want to thank J. Wagner and A. Wixforth for helpful discussions and K. Schwarz and J. Schleife for technical assistance. Continuous support by G. Weimann and P. Koidl, and the financial support by the Bundesministerium für Verteidigung are gratefully acknowledged. The work of F. S. is supported by USAF Contract No. F33615-95-C-5445.

[1] D. L. Smith and C. Mailhiot, J. Appl. Phys. **62**, 2545 (1987).
[2] J. L. Johnson, L. A. Samoska, A. C. Gossard, J. L. Merz, M. D. Jack, G. R. Chapman, B. A. Baumgratz, K. Kosai, and S. M. Johnson, J. Appl. Phys. **80**, 1116 (1996).
[3] F. Fuchs, U. Weimar, W. Pletschen, J. Schmitz, E. Ahlswede, M. Walther, J. Wagner, and P. Koidl, Appl. Phys. Lett. **71**, 3251 (1997).
[4] R. H. Miles, D. H. Chow, Y. H. Zhang, P. D. Brewer, and R. G. Wilson, Appl. Phys. Lett. **66**, 1921 (1995); J. R. Meyer, C. A. Hoffman, F. J. Bartoli, and L. R. Ram-Mohan, Appl. Phys. Lett. **67**, 757 (1995).
[5] U. Weimar, F. Fuchs, E. Ahlswede, J. Schmitz, W. Pletschen, N. Herres, and M. Walther, Mater. Res. Soc. Symp. Proc. **484**, 123 (1998).
[6] F. Fuchs, U. Weimar, E. Ahlswede, W. Pletschen, J. Schmitz, and M. Walther, Proc. SPIE **3287**, 14 (1998).
[7] J. Schmitz, J. Wagner, F. Fuchs, N. Herres, P. Koidl, and J. D. Ralston, J. Cryst. Growth **150**, 858 (1995).
[8] F. Szmulowicz, Superlattices Microstruct. **22**, 295 (1997); Phys. Rev. B **54**, 11539 (1996); **57**, 9081 (1998).
[9] P. Voisin, G. Bastard, and M. Voos, Phys. Rev. B **29**, 935 (1984).
[10] J. P. Ommagio, R. Wagner, J. R. Meyer, C. A. Hoffman, M. J. Yang, D. H. Chow, and R. H. Miles, Semicond. Sci. Technol. **8**, S112 (1993).
[11] J. K. Maan, ''Magnetic Quantization in Superlattices,'' in *Festkörperprobleme/Advances in Solid State Physics*, edited by P. Grosse (Vieweg, Braunschweig, 1987), p. 137.
[12] C. A. Hoffman, J. R. Meyer, E. R. Youngdale, F. J. Bartoli, and R. H. Miles, Appl. Phys. Lett. **63**, 2210 (1993).